Dynamic Stability of a Microgrid with an Active Load

Nathaniel Bottrell, *Student Member, IEEE,* Milan Prodanovic, *Member, IEEE,* and Timothy C Green, *Senior Member, IEEE*

Abstract

Rectifiers and voltage regulators acting as constant power loads form an important part of a microgrid's total load. In simplified form, they present a negative incremental resistance and beyond that, they have control loop dynamics in a similar frequency range to the inverters that may supply a microgrid. Either of these features may lead to a degradation of small-signal damping. It is known that droop control constants need to be chosen with regard to damping, even with simple impedance loads. Actively controlled rectifiers have been modelled in non-linear state-space form, linearised around an operating point, and joined to network and inverter models. Participation analysis of the eigenvalues of the combined system identified that the low-frequency modes are associated with the voltage controller of the active rectifier and the droop-controllers of the inverters. The analysis also reveals that when the active load DC-voltage controller is designed with large gains, the voltage controller of the inverter becomes unstable. This dependency has been verified by observing the response of an experimental microgrid to step changes in power demand. Achieving a well-damped response with a conservative stability margin does not compromise normal active rectifier design, but notice should be taken of the inverter-rectifier interaction identified.

Index Terms

Microgrids; Small-Signal Stability; Inverters; Constant Power Loads; Active Loads; Rectifiers.

Nathaniel Bottrell and Timothy C Green are with the Department of Electrical and Computer Engineering, Imperial College, London. E-mail: nathaniel.bottrell04@imperial.ac.uk; t.green@imperial.ac.uk. Milan Prodanovic is with IMDEA Energy Institute E-mail: milan.prodanovic@imdea.org;

This work was supported by a Power Networks Research Academy scholarship (http://www.theiet.org/about/scholarships-awards/pnra/). The PNRA is brought together by the IET and funded by four UK power network companies, EA Technology and the EPSRC.

I. Introduction

The presence of distributed generation (DG) in a distribution network creates the possibility of microgrid formation [1]. If a microgrid is formed, whether after a line outage or during planned maintenance, there is a need for the DG to respond to changes in load, and share the load such that the DG operate within their limits.

From the literature, the control approaches that enable the DG to share the load and remain within their operating limits, either involve a communications link or the use of a droop method. Communication approaches may involve a master-slave link, where the DG outputs are controlled using a dispatch signal [2]. If the master DG unit regulating the grid voltage is not functioning or does not have enough capacity, the microgrid may not satisfy voltage and frequency limits.

The use of a droop control method has the advantages of not requiring a communication link and allows DG to support microgrids irrespective of which sources are available. Droop control is a known method, and is reported in [3] [4] [5] [6]. However, inverter-interfaced DG operated with droop controllers have relatively complex and dynamic properties. To ensure stability, the small-signal model needs to be assessed.

It is known that in droop controlled microgirds, the low-frequency modes (oscillations that are represented by conjugate eigenvalue pairs) are associated with the droop controllers. The low frequency modes are most likely to be poorly damped, and at a risk of instability during operating point or parameter changes [6]. The droop controllers give rise to low frequency modes. This is because of their use of low-pass filters to reject harmonic and negative sequence disturbances from the power measurements. The filtered power measurements are used to determine the frequency references for the AC-voltage controllers of the inverters.

Many droop control strategies have been proposed to increase the damping of the low frequency modes during both steady-state operation and transient behaviour. Improvements include adjusting the droop parameters while the microgrid is functioning by the use of either an energy manager [7] or a grid-impedance estimation strategy [8]. Feed-forward terms have been proposed in [9] and using an inverter to imitate a voltage source with a complex finite-output impedance is proposed in [10]. Using proportional, integral, and derivative controllers within the droop calculation have been proposed in [11] [12] [13] [14].

For simplicity, this work will not consider the enhancements of droop-controller to improve stability and will only consider the simple droop controller, as presented in [6]. This is to identify whether, the influence of active loads within the microgrid decrease the poorly damped modes associated with the droop controllers. One possibility to further simplify the microgrid model, is to represent the inverters by only their low-frequency dynamics as in [15], and extended to larger system sizes in [16]. This modelling technique is valid if the system is not sensitive to the mid-frequency or high-frequency dynamics.

This work is important since published literature has mostly [6] [15] [16] considered microgrids with passive (i.e. impedance) loads, whereas microgrid implementations are likely to include significant proportions of loads with active front ends. Active front ends are used for providing regulated voltage buses to supply the final use equipment. By regulating a voltage buses, the active load may exhibit characteristics of constant power loads.

It is known that, in general, load dynamics interact with generation and may influence the stability of the network [17] and that mode damping is influenced by the load type. Constant impedance loads generally increase damping, whereas constant power loads tend to decrease damping [18]. To understand how a network responds to different generation technologies, in this case DG, the different load dynamics must be studied. The results produced from using only static loads may be misleading, since they might not represent the true demographic of loads connected to the network [19].

Constant power loads typically destabilise DC microgrid networks [20] [21] [22] and were shown to destabilise a microgrid in [23]. This paper concluded that constant power loads are only stable if paralleled with constant impedance loads. The study used the small-signal representation of an ideal constant power load, which exhibits a negative incremental resistance $\left(\Delta i = -\left(\frac{P}{V^2}\right)\Delta v\right)$ but this does not consider the dynamics of the bus regulator.

Large-signal stability of a microgrid, with various load types, was investigated in [24]. The conclusion from this was that constant PQ loads and impedance loads have no affect on stability, but motor loads do. Although this work did not consider small-signal stability, it is important because it demonstrates that constant power loads have the possibility of being stable without the need to be paralleled with constant impedance loads (contrary to the assertion in [23])

To determine network stability either eigenvalue analysis, or the Mapping Theorem as in [25], or impedance methods could be used. Impedance methods plot the source and load impedance as

a function of frequency. If the source impedance has a magnitude, as a function of frequency, that is greater than that of the load impedance, then the system will be unstable [26]. A development of this approach is in [27], where a root locus method was developed. Both these methods are useful tools in determining the system stability, but, unlike participation analysis, they don't lend themselves to determine the interactions between states.

The objective for the study reported here is to examine whether, first, the negative resistance characteristic of active front-end loads have a significant destabilizing effect on microgrids and, second, whether there are significant interactions between the dynamics of the inverters and the active loads such that their controllers need coordination or co-design.

The approach to be taken follows that of [6] and [28] by using full dynamic models of all elements. This is justified, since the separation of modes into distinct frequency groups (based on controller bandwidths) is still a matter of choice by the equipment designer. Each inverter and load is modelled on a local rotating (dq) reference frame and then the sub-systems are combined onto a common reference frame by the use of rotation functions. The models of inverters will be taken from [6] and models of the active load will be taken from [29]. A laboratory microgrid with three 10kVA inverters is used, as an example for, experimental verification of the analytical results.

Eigenvalue analysis will be used to assess the stability of the system, and the sensitivity to change in the gain of the DC-voltage controller of the active load. To determine interactions between the eigenvalues, participation analysis will be performed. Participation analysis allows the investigation of the sensitivity of eigenvalues to the states of the microgrid and indicates interactions between the dynamics of the inverters and the active load.

II. Modelling the Active Load in the Microgrid

A. Active Load Model

A switched-mode active rectifier is used in this study as an example of an active load supplying a regulated DC bus. The rectifier is modelled using an averaging method over the switching period, as in [30]. The chosen averaging method is based on the method developed by R. D. Middlebrook, which averages the circuit states [31]. Models can be readily developed by representing the switching elements as equivalent variable-ratio transformers [32].

Averaged models reflect the key dynamics of the system which are below the switching frequency. In general, the models are non-linear but can be linearised around an operating point. [33] [34]. With linear state-space representation, frequency domain analysis can be used to study the system stability.

State-space models of rectifiers that have been previously presented, have considered connection to a stiff-grid as in [35] but have not included the dynamics of frequency change. Not accounting for frequency change is a safe assumption when the active load is connected to a large grid or a single frequency source. In large networks, one active load will be a small percentage of the total loads and will not have enough of an effect on the network to cause a frequency disturbance. However, in a small microgrid with droop controllers, a load change from an active load could be a significant percentage of the total load and have a significant effect on the frequency. For this reason, the frequency of the network must be considered in the active load model.

Switch-mode active loads require an AC-side filter to attenuate switching frequency harmonics. The order and design of the filter varies, with higher order filters being more common in high power equipment. In the laboratory microgrid, the active load used an LCL filter rather than an LC filter. This offers higher attenuation with smaller passive components. However, lightly damped resonances of LC and LCL filters require careful design of the power converter control loops [35] [36].

An overview of the control system, for the example active load studied here, is shown in Fig. 1. The active load must be synchronized to the network voltage, commonly achieved with a phase-lock-loop. In modeling terms, the reference frame of the controller model is made synchronous with the local network voltage. Many different control structures are possible and work in [37] compares different PI current controllers, reviews their advantages, and presents methods of providing active damping. The use of a Linear Quadratic Regulator has also been reported [38]. For this study, a relatively simple structure was adopted and is shown in Fig. 2. All controllers use a PI regulator, and the outer DC bus voltage controller forms the reference for an inner current regulator. The inner current regulator is in dq form and regulates the AC-side currents flowing in the inductive element that is between the H-bridge and the AC-side capacitor. No active damping was incorporated, but it could be with a relatively simple extension to the model.

The current is defined according to a load convention. In a current controller of an inverter,

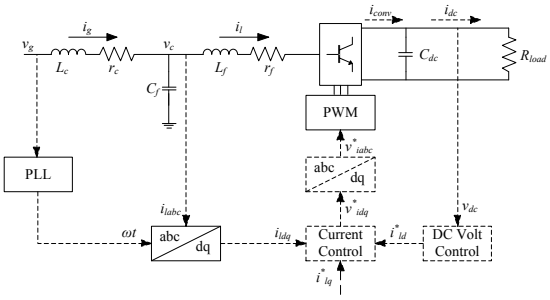

Fig. 1: Active Load Circuit

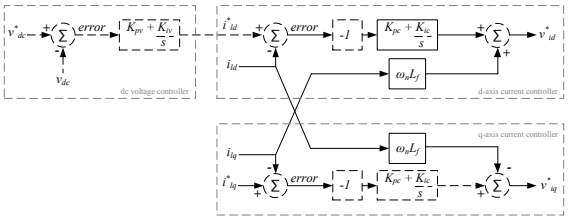

Fig. 2: Active Load DC voltage and AC current controller

where the current is defined positive when travelling from the H-bridge to the grid connection, the equation is Equ. 1 and Equ. 2. [6] [39]

$$v^*_{id} = -\omega_n L_f i_{lq} + K_{pc}\left(i^*_{ld} - i_{ld}\right) + K_{ic}\int\left(i^*_{ld} - i_{ld}\right)dt \tag{1}$$

$$v^*_{iq} = \omega_n L_f i_{ld} + K_{pc}\left(i^*_{lq} - i_{lq}\right) + K_{ic}\int\left(i^*_{lq} - i_{lq}\right)dt \tag{2}$$

However, positive current in the active load is defined as flowing from the grid connection to the H-bridge. This is the inverse direction of an inverter. To use the current controllers of the inverter in the active load and compensate for the reverse current direction, each current measurement needs to be multiplied by negative one. Performing this operation transforms the current controller of the inverter in Equ. 1 and Equ. 2 to a current controller of an active load in Equ. 3 and Equ. 4. This current controller is shown within Fig. 2. [29]

$$v^*_{id} = \omega_n L_f i_{lq} - K_{pc}\left(i^*_{ld} - i_{ld}\right) - K_{ic}\int\left(i^*_{ld} - i_{ld}\right)dt \tag{3}$$

$$v_{iq}^{*} = -\omega_n L_f i_{ld} - K_{pc}\left(i_{lq}^{*} - i_{lq}\right) - K_{ic}\int\left(i_{lq}^{*} - i_{lq}\right)dt \tag{4}$$

Transformation of the dq reference frame uses Equ. 5. Reference inputs to the controllers are indicated with a superscript asterisk. Upper-case 'D' and 'Q' have been used to denote variables on the common system reference frame of the microgrid. Lower-case 'd' and 'q' denote variables on the individual reference frame of a particular load or inverter.

$$[T_{dq}] = \sqrt{\frac{2}{3}}\begin{bmatrix} \cos(\omega t+\theta) & \cos\left(\omega t+\theta-\frac{2\pi}{3}\right) & \cos\left(\omega t+\theta+\frac{2\pi}{3}\right) \\ -\sin(\omega t+\theta) & -\sin\left(\omega t+\theta-\frac{3}{2\pi}\right) & -\sin\left(\omega t+\theta+\frac{3}{2\pi}\right) \\ \frac{1}{\sqrt{2}} & \frac{1}{\sqrt{2}} & \frac{1}{\sqrt{2}} \end{bmatrix}. \tag{5}$$

The model uses various frequency variables, these are $\omega, \omega_n, \omega_0$ and ω_{COM}. The variable ω denotes an arbitrary time varying frequency. Nominal system frequency, with a value of $2\pi 50$ in the example here, is denoted by ω_n. The initial frequency at time zero is donated by ω_0 and the common system reference frame frequency is denoted by ω_{COM}.

For simplicity, the model is split into constituent parts. The constituent parts are represented as linear state-space equations and then combined into a large state-space model. This process is presented in [29].

The model of the active load, required for the proposed system study, takes the AC network voltage as its input and returns the resulting AC network current as its output. The model has been divided into various subsystems, such as the DC bus regulator, AC current controller and the filter elements. The modelling of each of these, and their assembly into a complete model of the active load, is described in [29]. The resulting state-space model consists of a state-transition matrix A, matrices for inputs from the AC network voltage B_v, the common system frequency B_ω, and all other inputs B_u. The matrix C_c forms the AC current output, and the matrix C is used to observe other outputs during testing. The matrix D is the feed-forward matrix that couples input to output. Finally, a matrix M is used to define the network node, to which the active load model is connected, and also includes a high value resistive path to ground at each node which is there to define the node voltages.

B. Active Load in the Microgrid Model

The active load is connected to node three of the three-node example microgrid, which is depicted in Fig. 3. From the line parameters quoted in Fig. 3, it can be seen that the active load

is connected via a relatively long feeder. The active load was connected here because this is the weakest section of the microgird and is expected to show instabilities more readily. A simple microgrid was chosen in order to allow a laboratory test system to be built.

By using the method in [29], the matrices of the microgrid can be systematically built to represent any microgrid topology. The approach used in [29] can be used on higher dimension microgrid systems, and could be developed to identify the small-signal stability when integrating DG into the distribution network.

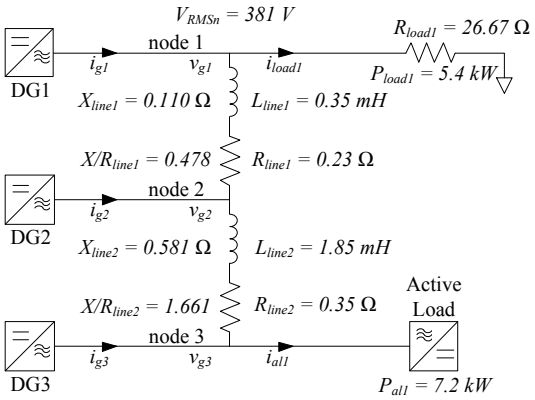

Fig. 3: Active Load Connected to Microgrid

The various subsystems of the example microgrid will be identified using the subscripts listed in Table I. Each of the subsystems modelled uses the procedure presented in [6]. [29] provides further information about how the components were incorporated into the microgrid.

One inverter is selected to provide the common system frequency, and this is represented in an extra matrix 'C_ω'. The inverter that is the common system frequency has a non-zero 'C_ω' matrix, whereas the other inverters have a zero 'C_ω' matrix. A disturbance component, not shown in Fig. 3, allows a current to be injected or drawn from any node.

The state-space model of the microgrid that incorporates the active load is summarized by Equ. 6, Equ. 7, and Equ. 8.

Component	Identifying subscript
Inverter	INV
Line	NET
Load	$LOAD$
Rectifier	REC
Disturbance	$DIST$

TABLE I: Subscripts for the Components in the Microgrid

$$A_{mg} = \begin{bmatrix} A_{INV} + B_{INVv}M_{INV}C_{INVc} + B_{INV\omega}C_{INV\omega} & B_{INVv}M_{NET}C_{NETc} & B_{INVv}M_{LOAD}C_{LOADc} & B_{RECv}M_{REC}C_{RECc} \\ B_{NETv}M_{INV}C_{INVc} + B_{NET\omega}C_{INV\omega} & A_{NET} + B_{NETv}M_{NET}C_{NETc} & B_{NETv}M_{LOAD}C_{LOADc} & B_{NETv}M_{REC}C_{RECc} \\ B_{LOADv}M_{INV}C_{INVc} + B_{LOAD\omega}C_{INV\omega} & B_{LOADv}M_{NET}C_{NETc} & A_{LOAD} + B_{LOADv}M_{LOAD}C_{LOADc} & B_{LOADv}M_{REC}C_{RECc} \\ B_{RECv}M_{INV}C_{INVc} + B_{REC\omega}C_{INV\omega} & B_{RECv}M_{NET}C_{NETc} & B_{RECv}M_{LOAD}C_{LOADc} & A_{REC} \\ +B_{RECv}M_{REC}C_{RECc} & & & \end{bmatrix}. \tag{6}$$

$$B_{mg} = \begin{bmatrix} B_{INVv}M_{DIST}C_{DISTc} & 0 \\ B_{NETv}M_{DIST}C_{DISTc} & 0 \\ B_{LOADv}M_{DIST}C_{DISTc} & 0 \\ B_{RECv}M_{DIST}C_{DISTc} & B_{RECu} \end{bmatrix}, \tag{7}$$

$$C_{mg} = \begin{bmatrix} C_{INV} & 0 & 0 & 0 \\ 0 & 0 & C_{LOAD} & 0 \\ 0 & 0 & 0 & C_{REC} \\ M_{INV}C_{INVc} & M_{NET}C_{NETc} & M_{LOAD}C_{LOADc} & M_{REC}C_{RECc} \end{bmatrix}, \; D_{mg} = \begin{bmatrix} 0 & 0 \\ 0 & 0 \\ 0 & 0 \\ M_{DIST}C_{DISTc} & 0 \end{bmatrix} \tag{8}$$

III. Identification of Mode Groups

Participation factors can provide a useful insight into what features of a system give rise to a given mode. The participation factor of the ith state and jth eigenvalue is defined as the product of the left eigenvectors (w_{ik}) and right eigenvectors (v_{ki}) [40]:

$$p_{ij} = \frac{|w_{ij}|\,|v_{ji}|}{\sum_{k=1}^{N}\left(|w_{ik}|\,|v_{ki}|\right)} \tag{9}$$

The participation matrix is a matrix of all the participation factors. The higher a particular participation factor, the more the state i participates in determining the mode j. Here the highest participation factor for each mode, will be used to identify that mode with a particular control subsystem within the microgrid. In this work, the function of the participation factor is to produce a state to mode mapping, and to identify parameters within the active load and microgrid that impact the modes of the system. Participation factors are a common tool for accessing the small-signal stability of networks and, as an example, have been used in [6] [41] [42].

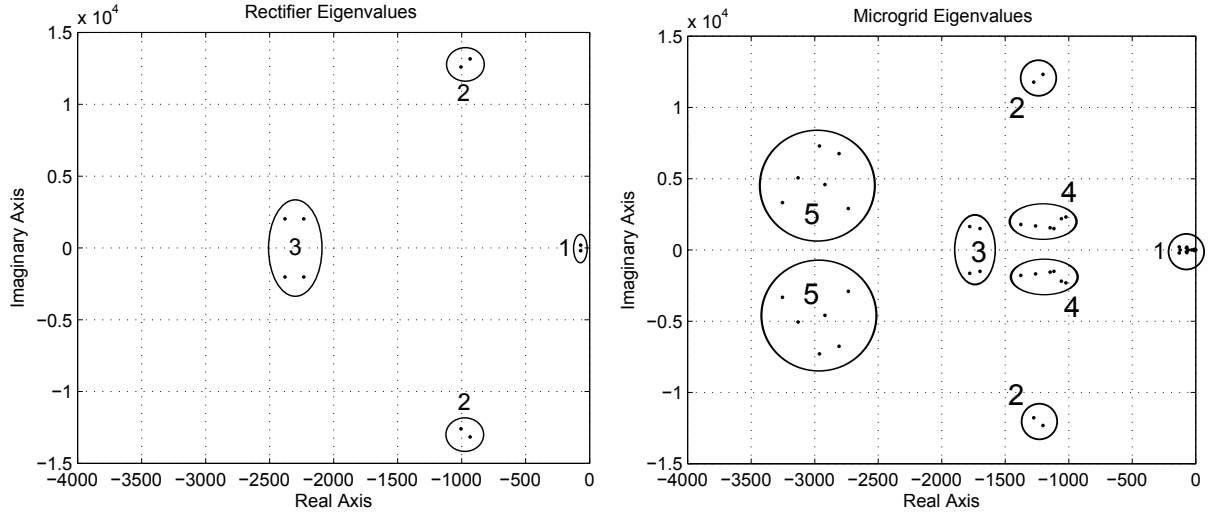

(a) Active Load

(b) Active Load in the Microgrid

Fig. 4: Eigenvalues of the Active Load and Active Load in the Micriogrid

A. Active Load Alone

Fig. 4 (a) shows the eigenvalue plot of the active load model, which is calculated from the active load A matrix. The group of modes labelled 1 in Fig. 4 (a), all have high participation factors for the states of the DC-side capacitor and the integrator of the DC bus-voltage regulator. The group labelled 2 are associated with the voltage of the AC-side capacitor C_f and the inductor L_c. The third group are associated with the integrator of the current controller and AC-side inductor L_f.

B. Active Load in Microgrid

When the eigenvalues of the complete system of the active load within a microgrid are considered, as shown in Fig. 4 (b), two further mode groups are identified. Groups 4 and 5 are similar to those found in [6] and are associated with the LCL filter, voltage controller and current controllers of the three inverters. In group 1, the low frequency modes associated with the active load's DC bus regulator, have been supplemented by the modes associated with the droop controllers of the inverters and so many more eigenvalues are present. A question that arises is whether the modes within group 1 are two independent subgroups or whether the modes are jointly influenced by the design of the inverters and the active loads.

By observing how the groups, associated with the active load, change from Fig. 4 (a) to Fig. 4 (b), an understanding of the effect of the microgrid on the rectifier can be obtained. All three groups appear to be in similar locations on Fig. 4 (a) and Fig. 4 (b), but closer inspection reveals that groups 2 and 3 have changed slightly. As already discussed, groups 2 and 3 in Fig. 4 are those associated with the LCL filter and the current controllers of the active load. Group 3 has become better damped (with the real part of the eigenvalue changing from approximately $-2,300$ to $-1,750$) and group 2 has become slightly less well damped ($-1,000$ to $-1,200$).

IV. Identification of Modes Showing Load-Inverter Coupling

Participation analysis not only reveals the states which dominate in formation of the mode, but can reveal second and subsequent influences. For a given set of states, the participation factors for each eigenvalue are summed and plotted on an x-y-z plot. The x-axis and the y-axis are the real and imaginary axes of the eigenvalue plot, and the z-axis is the participation for each eigenvalue. Eigenvalues that have higher participation of the selected states have a longer stem on the x-y-z plot. If more than one state is selected for analysis, then the participation value shown on the z-axis is a sum of all the participation values associated with the selected states.

Fig. 5 is a plot of the participation factors of the eigenvalues for the active load states only. The figure reveals the coupling between the active load and the inverters. It is observed that there is a small coupling between the active load and the eigenvalues in groups 4 and 5, which are strongly associated with the inverters. The small coupling is seen between the active load and the mid-frequency modes of the inverters, and also between the active load and the high-frequency

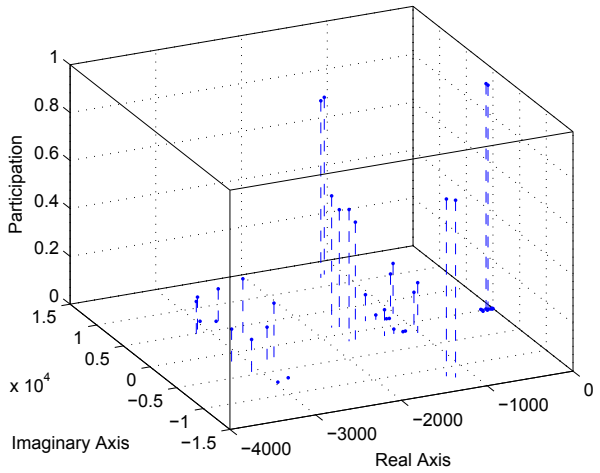

Fig. 5: Participation Analysis of the Active Load in the Microgrid

modes of the inverters. No coupling is observed between the active load and low-frequency modes of the inverters.

The conclusion from the coupling, is that the droop controllers of the inverters and the controllers of the active load are largely independent (at least for this example), and can be designed on that assumption. The participation analysis indicates a small coupling between the active load and the inverter voltage and current controllers. In order to ensure that the indicated modes are stable, there needs to be an element of co-design. Or at the least, design rules must be agreed that allow the two to be designed by independent parties. If this is not done, the addition of an active load with a certain control characteristics, could destabilise the network voltage control.

V. Microgrid Eigenvalue Trace

It has been shown that coupling exists between the active load and some inverter states (current and voltage controller states) for the example network, and with the nominal control gains. Now it is useful to test how damping of the various modes is changed by changes in the load controller parameters.

Fig. 6 shows eigenvalues for the case where the time constant of the DC bus voltage regulator $\frac{K_{pv}}{K_{iv}}$ was held constant at $\frac{1}{300}$, while the integral gain K_{iv} was varied from 15 to 2700 (the value used in the earlier plots was 150). It is seen that two eigenvalues move significantly. The first,

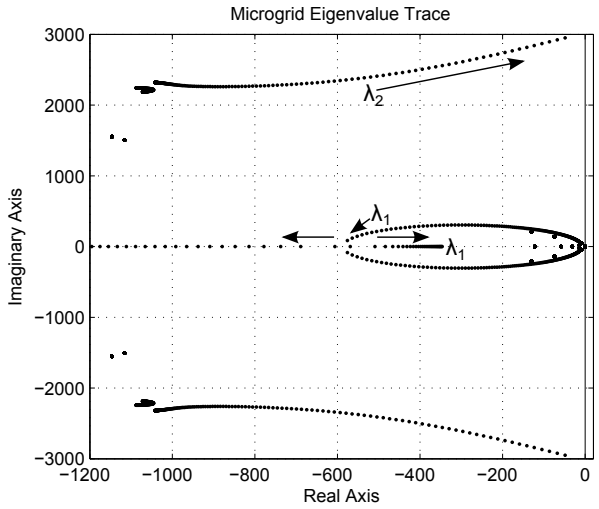

Fig. 6: Low Frequency Microgrid Eigenvalue Trace

trace of λ_1, are the low frequency modes associated with the DC-voltage controller of the active load, which one would expect to depend on K_{iv}. The second trace, λ_2, is of the modes associated with the AC-voltage controller of the inverters. The second trace shows that high gains in the load controller can lead to very low damping of the inverter voltage controller, and a risk of instability.

Fig. 6 also confirms the conclusions drawn from Fig. 5 about the coupling between the active load and inverters. The low frequency modes of the inverter droop controllers are not coupled to the active load. The evidence for this is that eigenvalues associated with the inverter droop controllers did not move when K_{iv} was changed. The active load is coupled with the mid-frequency modes of the inverters as already seen in Sec. IV, but beyond what was expected. It was not expected that changing the DC-voltage controller gains of the active load would have such an effect on the mid-frequency modes associated with the voltage controller of the inverter. To investigate this feature the participation values were plotted against gain.

Fig. 7 shows the participations of six states in eigenvalue λ_2 as a function of the gain K_{iv}. Four states from the inverter where chosen because they have the highest participation values at low gain. Two states from the active load are chosen, one state associated with the low-frequency modes and one state associated with the mid-frequency modes. All six states are identified in Table II. It is observed that the participation of the active load states grows rapidly as the gain

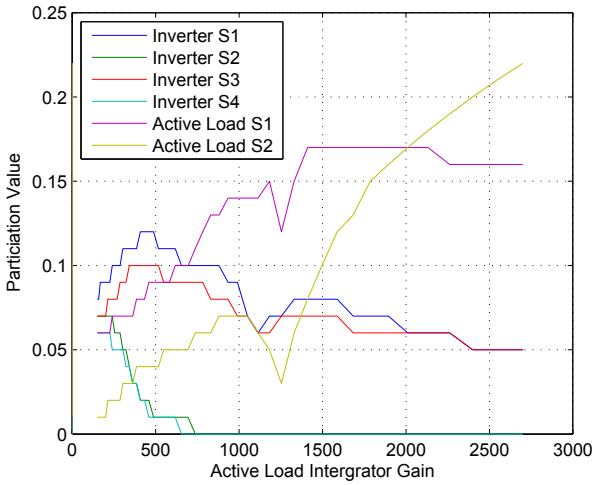

Fig. 7: Participation trace of 4 inverter states and 2 active load states as a function of the active load DC-voltage controller integral gain for the eigenvalue λ_2

State	Description
Inverter S1	Inverter 3 d-axis AC voltage controller state
Inverter S2	Inverter 3 q-axis AC voltage controller state
Inverter S3	Inverter 3 d-axis AC capacitor voltage state
Inverter S4	Inverter 3 q-axis AC capacitor voltage state
Active Load S1	Active Load d-axis AC current state
Active Load S2	Active Load DC capacitor voltage state

TABLE II: Description of the states plotted in Fig. 7

increases. Also, high gains in the DC-voltage controller of the active load cause a further coupling between the DC-voltage controller and AC-current controller of the active load. This informs us that the link between eigenvalues and states may change as the design parameters change. The participation factors only provide information about the system, and its couplings, for a fixed set of design parameters.

The eigenvalue trace in Fig. 6 confirms the results shown in the participation analysis. It can be concluded that the low-frequency modes of the active load do not couple with the low-frequency modes of the inverters. However, there is coupling between the low-frequency modes of the active load and the mid-frequency modes of the inverters when the active load has high gains in the DC-voltage controller. These couplings must be considered when designing a microgrid with

active load.

VI. Experimental Results

The example microgrid of Fig. 3 was available for experimental testing. It was equipped with three 10 kVA inverters operating as droop-controlled sources with a nominal line voltage of 381 V. The active load was provided by another inverter with a further power converter for removing power from the DC bus. Tests at two different gains were conducted to illustrate the results. In each, the power consumption of the active load is stepped from $5,900$ W to $8,000$ W and the transient response of the load's DC bus voltage, the inverters' output powers and the inverter's d-axis voltage were observed. The gains used, detailed in Table III, correspond to the nominal gains used in the initial analysis and the extremes of the gain range used in Fig. 6. The purpose of the experimental work is to validate the relationship between the active load and the microgrid that were found from the participation analysis.

Test Name	K_{iv}	K_{pv}	$\tau = \frac{K_{pv}}{K_{iv}}$
Nominal Gain	150	0.5	1/300
High Gain	2700	9	1/300

TABLE III: Gains of DC Bus Voltage Regulator of the Active Load

A. Transient response with nominal gain

In this experiment, the low-frequency modes of the microgrid observed in the time domain, are compared to the eigenvalue plot. In Fig. 8 (a) two modes are identified. The mode with a frequency of 32 Hz and a damping factor of 0.347 is associated with the DC voltage controller and DC capacitor of the active load. The mode with a frequency of 4.12 Hz and a damping factor of 0.534 is associated with the droop controllers of the inverters.

Fig. 8 (b) shows that when the load is stepped, the DC voltage oscillates with a frequency of 30.3 Hz and has a damping factor of 0.25. The envelope of the damping factor is shown by the black long-dash line. The experimental damping factor is slightly less than the model predicts and the frequency observed is in reasonable agreement with the model.

Fig. 8 (c) shows that the three inverters, which have identical droop settings, share the increased power equally when the new steady-state is established. The initial increase in power is all taken

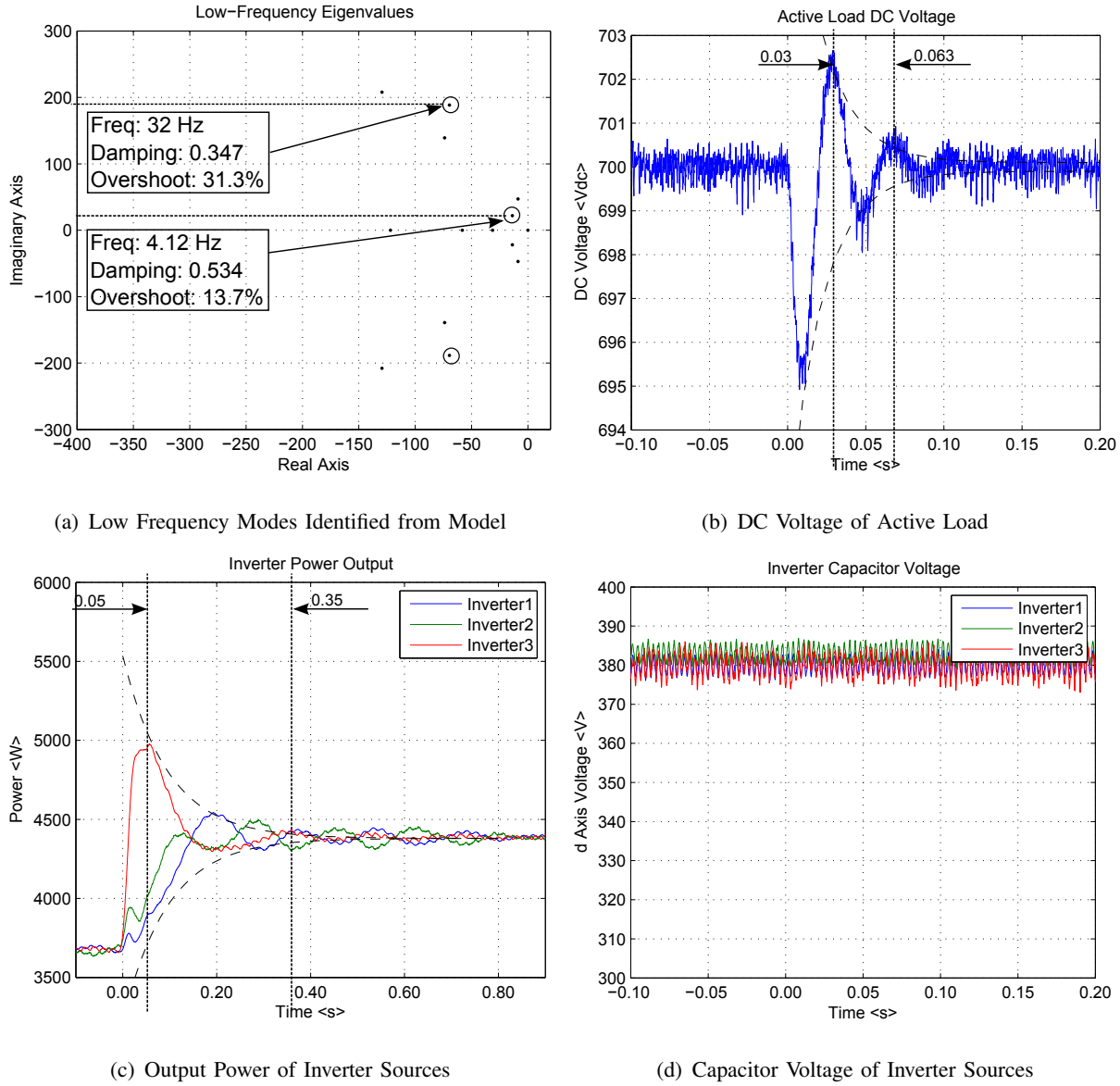

(a) Low Frequency Modes Identified from Model

(b) DC Voltage of Active Load

(c) Output Power of Inverter Sources

(d) Capacitor Voltage of Inverter Sources

Fig. 8: Experimental Results with Nominal Gain and Active Load Operating Point of 5 kW

by inverter 3, which is electrically closest to the load where the power step occurred. The transient of the power output from inverter 3 has a frequency of 3.33 Hz and has a damping factor of 0.5. The damping factor envelope is shown by the black long-dash line. The observed frequency and damping factor are in reasonable agreement with the model.

Fig. 8 (d) shows the d-axis capacitor voltage of the inverter sources. The power step of the active load change has not caused a noticeable transient in the voltage trace. This figure confirms

stable operation of the microgrid when the active load is increased.

B. Transient response with high gain

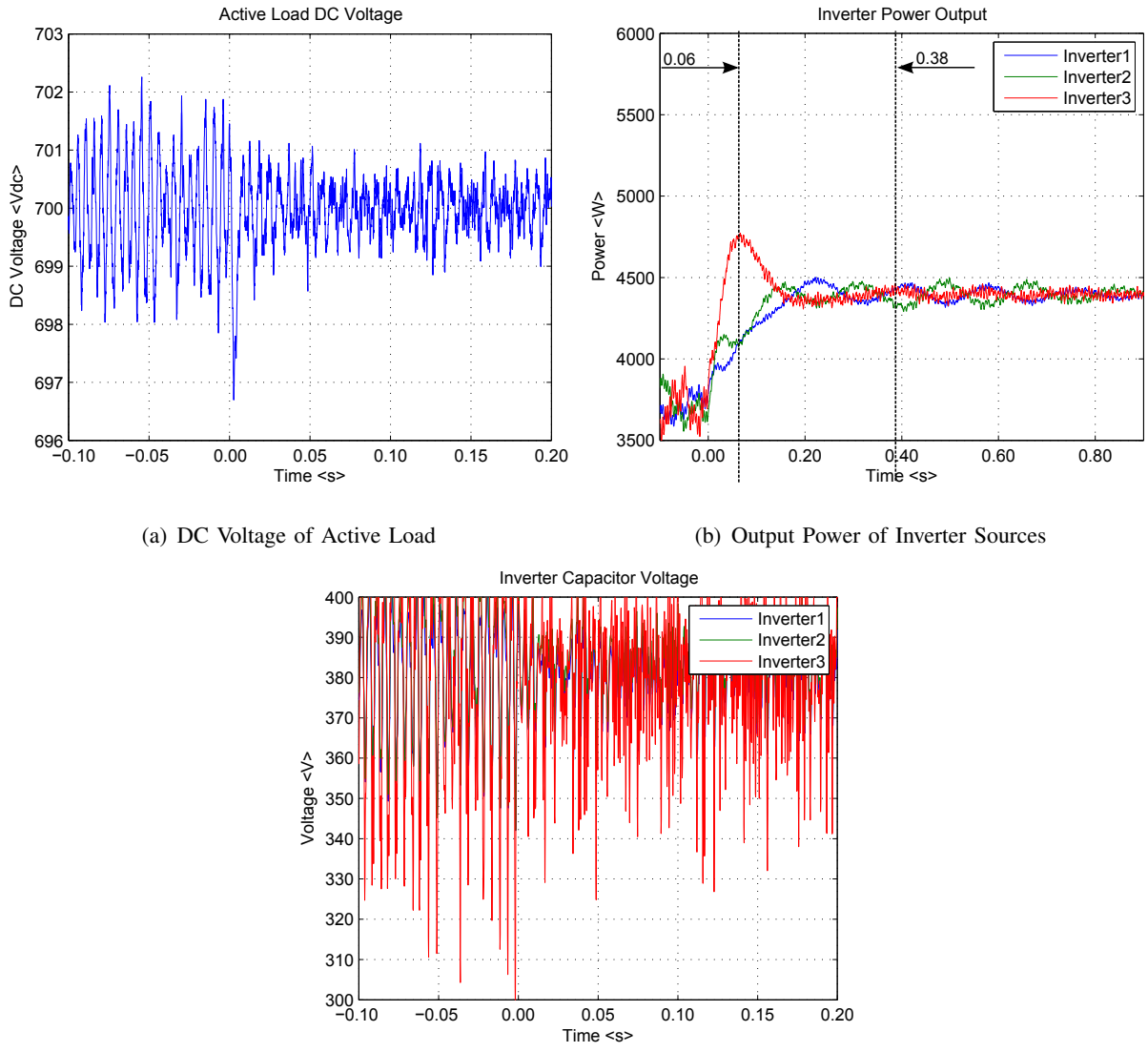

(a) DC Voltage of Active Load

(b) Output Power of Inverter Sources

(c) Capacitor Voltage of Inverter Sources

Fig. 9: Experimental Results with High Gain

The experiment in Sec. VI-A was repeated for a higher gain in the DC-voltage controller of the active load. The participation analysis of the microgrid with a high gain in the DC-voltage controller of the active load, showed a link between the active load DC-voltage controller and

the inverters' voltage controller. The eigenvalue sweep showed that the eigenvalues, originally associated with the voltage controller of the inverter, becoming unstable and also showed the low frequency eigenvalues remaining stable.

Fig. 9 (a) shows the DC voltage of the active load. The DC voltage is more oscillatory than at nominal gain but that reduces slightly after the load power increases. At the instant of load change, the low frequency transient is not present. This change was observed by the change in position of eigenvalue λ_1 in Fig. 6.

Fig. 9 (b) shows the droop controller power output of the inverters. The droop controllers have remained stable and are at a frequency of 3.1 Hz. This is a very slight change from the output of the droop controllers in the nominal gain case. The eigenvalue plot in Fig. 6 showed the low frequency modes, associated with the droop controllers, to be unaffected by the gain change.

Fig. 9 (c) shows the capacitor voltage of the inverters. The gains in the inverter have not altered, yet the voltage highly oscillatory. Increasing the gain in the DC voltage controller of the load has caused the microgrid to become unstable. It is clear that this experimental test confirms the link seen in the eigenvalue trace, where the mid-frequency modes of the inverters move and become coupled with the active load when the gain of the active load DC-voltage controller is increased.

VII. Conclusion

This paper has used a model of an active load [29] as part of a simple 3-node microgrid using the same framework as [6]. The active load was modelled as a non-linear state-space model which was joined to a microgrid, with similar models of droop-controlled inverters and a network, using a common reference frame. The model was linearised about an operating point, and participation analysis was used to identify which state variables were associated with which eigenvalues. The low frequency eigenvalues, that are associated with either the inverter droop controllers or the DC-voltage controller of the active load, had little interaction. In contrast, a medium-frequency eigenvalue, that was initially associated with the AC-voltage controller of the inverters, became much less damped when the gain of the active load DC-voltage controller was increased.

The system model has been verified against an experimental system with three 10 kVA inverters, one passive load and one active load. Step changes of load were used to excite low-frequency

modes and allow observation of frequency and damping factor for two controller gain conditions. Despite initial concerns that the negative resistance property of constant power loads would destabilise the power-sharing (droop) controllers, no significant reduction of damping of the low frequency modes was observed for a range of active load voltage control parameters. However, the eigenvalue analysis showed that, eigenvalues associated with the DC-voltage controller of the active load moved away from the imaginary axis and the eigenvalues associated with the inverter AC-voltage controller moved towards the imaginary axis as the gains of the rectifier DC-voltage controller were varied. The degradation of damping of this mode was observed in the experiments also.

Although some inverter-rectifier coupling has been identified, it was not in the low-frequency power sharing eigenvalues as anticipated. In the example experimental system, unstable operation did occur for very large gains in the DC voltage loop but these were beyond the gains needed to achieve good steady-state voltage regulation. Therefore it is possible to design the rectifier controller by using conventional frequency domain analysis and independently of the inverter controllers, provided the design is suitably conservative.

ACKNOWLEDGMENT

The authors would like to thank Dr R. Silversides who has provided much support in setting up the experimental equipment.

REFERENCES

[1] R. H. Lasseter, "Microgrids and Distributed Generation," *Journal of Energy Engineering*, vol. 133, no. 3, pp. 144–149, Sep. 2007.

[2] B. Bahrani, H. Karimi, and R. Iravani, "Decentralized control of parallel connection of two distributed generation units," *Industrial Electronics, 2009. IECON '09. 35th Annual Conference of IEEE*, pp. 358 –362, nov. 2009.

[3] M. Chandorkar, D. Divan, and R. Adapa, "Control of Parallel Connected Inverters in Standalone AC Supply Systems," *IEEE Transactions on Industry Applications*, vol. 29, no. 1, pp. 136–143, Jan. 1993.

[4] E. Coelho, P. Cortizo, and P. Garcia, "Small-signal stability for parallel-connected inverters in stand-alone ac supply systems," *Industry Applications, IEEE Transactions on*, vol. 38, no. 2, pp. 533 –542, mar/apr 2002.

[5] F. Gao and M. Iravani, "A Control Strategy for a Distributed Generation Unit in Grid-Connected and Autonomous Modes of Operation," *Power Delivery, IEEE Transactions on*, vol. 23, no. 2, pp. 850 –859, april 2008.

[6] N. Pogaku, M. Prodanovic, and T. C. Green, "Modeling, Analysis and Testing of Autonomous Operation of an Inverter-Based Microgrid," *IEEE Transactions on Power Electronics*, vol. 22, no. 2, pp. 613–625, Mar. 2007.

[7] E. Barklund, N. Pogaku, M. Prodanovic, C. Hernandez-Aramburo, and T. Green, "Energy management in autonomous microgrid using stability-constrained droop control of inverters," *Power Electronics, IEEE Transactions on*, vol. 23, no. 5, pp. 2346 –2352, sept. 2008.

[8] J. Vasquez, J. Guerrero, A. Luna, P. Rodriguez, and R. Teodorescu, "Adaptive droop control applied to voltage-source inverters operating in grid-connected and islanded modes," *Industrial Electronics, IEEE Transactions on*, vol. 56, no. 10, pp. 4088 –4096, oct. 2009.

[9] M. Delghavi and A. Yazdani, "An adaptive feedforward compensation for stability enhancement in droop-controlled inverter-based microgrids," *Power Delivery, IEEE Transactions on*, vol. 26, no. 3, pp. 1764 –1773, july 2011.

[10] K. De Brabandere, B. Bolsens, J. Van den Keybus, A. Woyte, J. Driesen, and R. Belmans, "A voltage and frequency droop control method for parallel inverters," *Power Electronics, IEEE Transactions on*, vol. 22, no. 4, pp. 1107 –1115, july 2007.

[11] J. Guerrero, N. Berbel, J. Matas, L. de Vicuna, and J. Miret, "Decentralized control for parallel operation of distributed generation inverters in microgrids using resistive output impedance," in *IEEE Industrial Electronics, IECON 2006 - 32nd Annual Conference on*, nov. 2006, pp. 5149 –5154.

[12] F. Katiraei and M. Iravani, "Power management strategies for a microgrid with multiple distributed generation units," *Power Systems, IEEE Transactions on*, vol. 21, no. 4, pp. 1821 –1831, nov. 2006.

[13] J. Kim, J. Guerrero, P. Rodriguez, R. Teodorescu, and K. Nam, "Mode adaptive droop control with virtual output impedances for an inverter-based flexible ac microgrid," *Power Electronics, IEEE Transactions on*, vol. 26, no. 3, pp. 689 –701, march 2011.

[14] M. Hua, H. Hu, Y. Xing, and J. Guerrero, "Multilayer control for inverters in parallel operation without intercommunications," *Power Electronics, IEEE Transactions on*, vol. 27, no. 8, pp. 3651 –3663, aug. 2012.

[15] M. Marwali, J.-W. Jung, and A. Keyhani, "Stability Analysis of Load Sharing Control for Distributed Generation Systems," *Energy Conversion, IEEE Transactions on*, vol. 22, no. 3, pp. 737–745, Sep. 2007.

[16] S. Iyer, M. Belur, and M. Chandorkar, "A Generalized Computational Method to Determine Stability of a Multi-inverter Microgrid," *Power Electronics, IEEE Transactions on*, vol. 25, no. 9, pp. 2420–2432, Sep. 2010.

[17] I. Hiskens and J. Milanovic, "Load Modelling in Studies of Power System Damping," *IEEE Transactions on Power Systems*, vol. 10, no. 4, pp. 1781–1788, Nov. 1995.

[18] M. Kent, W. Schmus, F. McCrackin, and L. Wheeler, "Dynamic Modeling of Loads in Stability Studies," *IEEE Transactions on Power Apparatus and Systems*, vol. PAS-88, no. 5Part-I, pp. 756–763, May 1969.

[19] E. Kyriakides and R. G. Farmer, "Modeling of Damping for Power System Stability Analysis," *Electric Power Components and Systems*, vol. 32, no. 8, pp. 827–837, Aug. 2004.

[20] A. Kwasinski and C. Onwuchekwa, "Dynamic behavior and stabilization of dc microgrids with instantaneous constant-power loads," *Power Electronics, IEEE Transactions on*, vol. 26, no. 3, pp. 822 –834, march 2011.

[21] M. Cespedes, L. Xing, and J. Sun, "Constant-power load system stabilization by passive damping," *Power Electronics, IEEE Transactions on*, vol. 26, no. 7, pp. 1832 –1836, july 2011.

[22] D. Marx, P. Magne, B. Nahid-Mobarakeh, S. Pierfederici, and B. Davat, "Large signal stability analysis tools in dc power systems with constant power loads and variable power loads; a review," *Power Electronics, IEEE Transactions on*, vol. 27, no. 4, pp. 1773 –1787, april 2012.

[23] D. Ariyasinghe and D. Vilathgamuwa, "Stability Analysis of Microgrids with Constant Power Loads," *Sustainable Energy Technologies, 2008. ICSET 2008. IEEE International Conference on*, pp. 279 –284, Nov. 2008.

[24] N. Jayawarna, X. Wu, Y. Zhang, N. Jenkins, and M. Barnes, "Stability of a MicroGrid," *Power Electronics, Machines and Drives, 2006. The 3rd IET International Conference on*, pp. 316–320, Mar. 2006.

[25] B. Bahrani, H. Karimi, and R. Iravani, "Stability analysis and experimental validation of a control strategy for autonomous operation of distributed generation units," *Power Electronics Conference (IPEC), 2010 International*, pp. 464 –471, june 2010.

[26] X. Feng, Z. Ye, K. Xing, F. Lee, and D. Borojevic, "Individual load impedance specification for a stable DC distributed power system," *Applied Power Electronics Conference and Exposition, 1999. APEC '99. Fourteenth Annual*, vol. 2, pp. 923 –929 vol.2, mar 1999.

[27] B. Bitenc and T. Seitz, "Optimizing DC power distribution network stability using root locus analysis," *Telecommunications Energy Conference, 2003. INTELEC '03. The 25th International*, pp. 691 –698, oct. 2003.

[28] A. Tabesh and R. Iravani, "Multivariable Dynamic Model and Robust Control of a Voltage-Source Converter for Power System Applications," *Power Delivery, IEEE Transactions on*, vol. 24, no. 1, pp. 462 –471, jan. 2009.

[29] T. Bottrell, N. Green, "Modelling Microgrids with Active Loads," *COMPEL 2012*, pp. 358 –362, jun. 2012.

[30] S. Sanders and G. Verghese, "Synthesis of Averaged Circuit Models for Switched Power Converters," *Circuits and Systems, IEEE Transactions on*, vol. 38, no. 8, pp. 905–915, Aug. 1991.

[31] R. D. Middlebrook and S. Cuk, "A General Unified Approach to Modelling Switching-Converter Power Stages," *International Journal of Electronics*, vol. 42, no. 6, pp. 521–550, Jun. 1977.

[32] C. Rim, D. Hu, and G. Cho, "The Graphical D-Q Transformation of General Power Switching Converters," *Industry Applications Society Annual Meeting, 1988., Conference Record of the 1988 IEEE*, vol. 1, pp. 940–945, Oct. 1988.

[33] S. Sudhoff, S. Glover, P. Lamm, D. Schmucker, and D. Delisle, "Admittance Space Stability Analysis of Power Electronic Systems," *IEEE Transactions on Aerospace and Electronic Systems*, vol. 36, no. 3, pp. 965–973, Jul. 2000.

[34] I. Jadric, D. Borojevic, and M. Jadric, "Modeling and Control of a Synchronous Generator with an Active DC Load," *IEEE Transactions on Power Electronics*, vol. 15, no. 2, pp. 303–311, Mar. 2000.

[35] M. Liserre, F. Blaabjerg, and S. Hansen, "Design and Control of an LCL-Filter-Based Three-Phase Active Rectifier," *Industry Applications, IEEE Transactions on*, vol. 41, no. 5, pp. 1281–1291, Sep. 2005.

[36] V. Blasko and V. Kaura, "A Novel Control to Actively Damp Resonance in Input LC Filter of a Three Phase Voltage Source Converter," *Applied Power Electronics Conference and Exposition, 1996. APEC '96. Conference Proceedings 1996., Eleventh Annual*, vol. 2, pp. 545–551, Mar. 1996.

[37] B.-H. Kwon, J.-H. Youm, and J.-W. Lim, "A Line-Voltage-Sensorless Synchronous Rectifier," *Power Electronics, IEEE Transactions on*, vol. 14, no. 5, pp. 966 –972, Sep. 1999.

[38] S. Alepuz, J. Bordonau, and J. Peracaula, "A Novel Control Approach of Three-Level VSIs Using a LQR-Based Gain-Scheduling Technique," *Power Electronics Specialists Conference, 2000. PESC 00. 2000 IEEE 31st Annual*, vol. 2, pp. 743 –748 vol.2, Jun. 2000.

[39] S. Yang, Q. Lei, F. Peng, and Z. Qian, "A Robust Control Scheme for Grid-Connected Voltage-Source Inverters," *Industrial Electronics, IEEE Transactions on*, vol. 58, no. 1, pp. 202 –212, jan. 2011.

[40] J. B. J. Machowski and J. Bumby, *Power System Dynamics: Stability and Control*. Wiley, 2008.

[41] A. Ostadi, A. Yazdani, and R. Varma, "Modeling and Stability Analysis of a DFIG-Based Wind-Power Generator Interfaced With a Series-Compensated Line," *Power Delivery, IEEE Transactions on*, vol. 24, no. 3, pp. 1504 –1514, july 2009.

[42] S. Balathandayuthapani, C. S. Edrington, S. D. Henry, and J. Cao, "Analysis and Control of a Photovoltaic System: Application to a High-Penetration Case Study," *Systems Journal, IEEE*, vol. 6, no. 2, pp. 213 –219, june 2012.

Nathaniel Bottrell (S'10) received the M.Eng. degree in Electrical and Electronic Engineering from Imperial College, London, UK., in 2009 and is currently pursuing the Ph.D. degree in Electrical and Electronic Engineering at Imperial College, London, UK.

His research interests include distributed generation, microgrids and the application of power electronics to low-voltage power systems.

Milan Prodanovic (M'01) received the B.Sc. degree in electrical engineering from the University of Belgrade, Belgrade, Serbia, in 1996 and the Ph.D. degree from Imperial College, London, U.K., in 2004.

Milan Prodanovic received a B.Sc. degree in Electrical Engineering from University of Belgrade, Serbia in 1996 and a Ph.D. degree from Imperial College, UK in 2004. From 1997 to 1999 he was engaged with GVS engineering company, Serbia, developing UPS systems. From 1999 until 2010 he was a research associate in the Control and Power Group at Imperial College in London. Currently he is a Senior Researcher and Head of the Electrical Processes Unit at IMDEA Energa Institute, Madrid, Spain. His research interests are in design and control of power electronics converters, RT control systems, micro-grids and distributed generation.

Timothy C. Green (M'89-SM'02) received the B.Sc. degree (first class honours) in electrical engineering from Imperial College, London, U.K., in 1986 and the Ph.D. degree in electrical engineering from Heriot-Watt University, Edinburgh, U.K., in 1990.

He was a Lecturer at Heriot Watt University until 1994 and is now a Professor of Electrical Power Engineering at Imperial College London and Deputy Head of the Control and Power Research Group. His research interest is in using power electronics and control to enhance power quality and power delivery. This covers interfaces and controllers for distributed generation, micro-grids, active distribution networks, FACTS and active power filters. He has an additional line of research in power MEMS and energy scavenging.

Prof. Green is a Chartered Engineer in the U.K. and MIEE.